2021 43rd Annual International Conference of the
IEEE Engineering in Medicine & Biology Society (EMBC)
Oct 31 - Nov 4, 2021. Virtual Conference

Application of correlated component analysis to dynamic PET time-activity curves denoising

Paulus Kapundja Shigwedha, Takahiro Yamada, Kohei Hanaoka, Kazunari Ishii, Yuichi Kimura, *Member, IEEE*, and Yutaka Fukuoka, *Member, IEEE*

***Abstract*— Positron emission tomography (PET) is a physiological, non-invasive imaging technique, which forms an essential part of nuclear medicine. The data obtained in a PET scan represent the concentration of an administered radiotracer in tissues over time. Quantitative analysis of PET data makes possible the assessments of *in-vivo* physiological processes. The Logan graphical analysis (LGA) is one of the methods that are used for quantitative analysis of PET data. LGA transforms PET data into a simple linear relationship. The slope of the LGA linear relationship is a physiological quantity denoting receptor availability. This quantity is termed distribution volume ratio (*DVR*). LGA-based estimates of the *DVR* are negatively affected by the noise in PET data —leading to the *DVR* being underestimated. A number of approaches proposed to address this issue have been observed to reduce the bias at the cost precision. An alternative regression method, least-squares cubic (LSC), was recently applied to estimate the *DVR* in order to reduce the bias. LSC was observed to reduce the bias in the LGA-based estimates. However, slight increases were also observed in the variance of the LSC-based estimates. This calls for methods to act against the variance in the LSC-based estimates. In this study, an alternative method is applied for tTAC denoising. This method is referred to as correlated component analysis (CorrCA). CorrCA transform the data by searching for dimensions of maximum correlation. This technique is closely related to other well-known methods such as principal component analysis and independent component analysis. In this study, the data were denoised by CorrCA (to act against the variance in the estimate) and the *DVR* was estimated by LSC, which provides for minimal bias. The resulting method LSC-CorrCA, gave less-biased estimated with increased precision. This was observed for both simulation results as well as for clinical data, both for ^{11}C Pittsburgh compound B. Simulation data revealed reduced variances in LCS-CorrCA-based estimates, and the clinical data showed improved contrast between gray and white matter regions.**

***Clinical Relevance*— Improved *DVR* estimates would ease the interpretation of medical images, which will in turn positively influence the clinical processes, from diagnosis to treatment and follow-ups.**

I. Introduction

In this study we introduce an alternative technique for smoothing positron emission tomography (PET) data, prior to Logan graphical analysis (LGA).

Logan graphical analysis (LGA) is a well-known technique used for quantitative analysis of dynamic positron emission tomography (PET) data, for radiotracers that bind reversibly [1, 2, 3]. LGA can be referred to as a linearization technique. It takes PET tissue time-activity curves (tTACs) data and transform them into a two-variables linear relationship. The slope of this linear relationship is referred to as distribution volume ratio (*DVR*). *DVR* denotes the availability of target receptor, and can be defined as the ratio of distribution volume in a receptor-containing to non-receptor region [2].

LGA has been noted to be efficient in terms of both time and computing, for which it has been well accepted [3]. However, for noisy PET data, LGA estimates have been shown to be negatively biased [3, 4]. This noise-induced bias has been shown to increases with the magnitude of both the noise and the *DVR* [5].

Different approaches have been proposed to address the LGA bias problem [6, 7, 8, 9]. Most notably, these methods reduce the bias at the expense of precision. Recently, we applied a new approach —least-squares cubic (LSC)— for bias reduction in [10], and compared it to the ordinary least-squares (OLS)-based LGA as well as the multilinear reference tissue model 2 (MRTM2) [8]. The LSC method performed better than both OLS and MRTM2 methods. LSC is a simple and direct approach; it simply replaces OLS with LSC to estimate the LGA slope parameter, the *DVR*. The specific details of the LSC regression method can be found in [11, 12, 13]. The LSC-based LGA reduces the bias in the *DVR* estimates because it accounts for errors in both the predictor and response variables [10]. This aspect of LSC is well suitable for the LGA variables, because both the predictor and response variables of the LGA are noisy. It was however, observed that the LSC approach also caused a slight decrease in precision, observed in terms of slightly increased variance in the estimates.

To minimize the influence of increased variance on the image quality, in this study we employed a tTAC denoising technique, Correlated component analysis (CorrCA) [14]. CorrCA is a relatively new method for feature extraction and dimension reduction, and to the best of our knowledge has never been previously applied to quantification of *in-vivo* radiotracer binding. In this approach, tTAC data are denoised

P. K. Shigwedha and Y. Fukuoka (corresponding author fukuoka@cc.kogakuin.ac.jp) are with the Department of Electrical Engineering and Electronics, Graduate School of Engineering, Kogakuin University, Shinjuku, Tokyo, Japan.

T. Yamada, and K. Hanaoka are with the Division of Positron Emission Tomography, Institute of Advanced Clinical Medicine, Kindai University, Osakasayama, Osaka, Japan.

K. Ishii is with the Department of Radiology, Faculty of Medicine, Kindai University, Osakasayama, Osaka, Japan.

Y. Kimura is with the Department of Computational Systems Biology, Faculty of Biology-Oriented Science and Technology, Kindai University, Kinokawa, Wakayama, Japan.

978-1-7281-1178-0/21/$31.00 ©2021 IEEE

by CorrCA and the *DVR* is estimated by LSC. Henceforth, we thus refer to this method as LSC–CorrCA.

The results obtained from the LSC–CorrCA method were compared to those of the LSC on its own, as well as the OLS-based LGA. The results were compared in terms of bias and variance in the *DVR* estimates for simulation results data. Clinical data were compared in terms of contrast between grey and white matter of ^{11}C Pittsburgh compound B (^{11}C-PiB) binding to beta amyloid (Aβ) plaques.

II. METHOD

A. Logan graphical analysis

By applying differential calculus to PET data, the LGA [1] can be obtained in the form of the equation below;

$$\frac{\int_0^t C(u)du}{C(t)} = DVR\left\{\frac{\int_0^t C^R(u)du}{C(t)}\right\} + int. \qquad (1)$$

The terms $C(t)$ and $C^R(t)$ in (1), represents the radioactivity in a tissue of interest and the reference tissue, respectively. The tissue of interest consists of the target receptors. On the other hand, the reference tissue is such that it has a negligible volume of target receptors.

Term int in (1) becomes constant against time after some time t^*. Consequently, (1) turns into a simple linear relationship between the two fraction terms, with slope *DVR*.

The use of a linear regression method on (1) will then allow for the estimate of the slope parameter *DVR*. In this study, the LSC regression method is employed.

A. Correlated component analysis

CorrCA is also a feature extraction method. CorrCA operates by identifying components that are maximally correlated between repetitions in multivariate data [14]. Specifically, CorrCA maximizes the ratio of "between-repetition to within-repetition" covariance. In the context of our application to PET data, our repetitions are along the slices dimension. CorrCA will therefore maximize the ratio of between-slices to within-slices covariance. This ratio is referred to as inter-subject correlation (ISC) [14]. Specifically in our context, it translates to inter-slice correlation.

Consider a set of dynamic PET brain volume data arranged as an array of size $q \times p \times M$, where M denotes the number of slices, q denotes the number of voxels in a slice, and p denotes the number of time points (frame numbers). CorrCA identifies directions in the p-dimensional space along which the tTACs maximally correlate between M slices, with correlation measured across q voxels.

CorrCA is closely related to the well-known principal component analysis (PCA). Let us put it into perspective in comparison to PCA applied to the same data. For the PCA case, we can represent the brain volume as an $R \times p$ array, where $R = q * M$, denotes the total number of voxels in the whole brain volume. PCA returns a set of p-dimensional vectors which successively capture the variance in the data in a descending order. Similarly, CorrCA returns a set p-dimensional vectors which successively capture the ISC in a descending order. CorrCA also formulates into an eigenvalues and eigenvectors problem, from which the p-dimensional orthogonal vectors (and correlated components) are found as the eigenvectors, and ISCs as the eigenvalues. Maximizing the between-slices to within-slices covariance maximizes the mean-over-variance across slices, which has been asserted to define a signal-to-noise ratio [14].

For a brief mathematical outline of CorrCA as presented in [14], let the observed noisy tTACs be, $x_i^j = \left[c_i^j(t_1), c_i^j(t_2), \cdots, c_i^j(t_p)\right]^T$, where $i = 1, 2, \ldots, q$ and $j = 1, 2, \ldots, M$. (^{T} denotes a transpose). Thus, $x_i^j \in \mathbb{R}^{p\times 1}$ is the i^{th} voxel in the j^{th} slice. This voxel can be represented as,

$$x_i^j(t) = Ay_i^j + \varepsilon_i^j, \qquad (2)$$

where $A \in \mathbb{R}^{p\times k}$ $(k \leq p)$ is a projection matrix to be constructed by CorrCA; $y_i^j \in \mathbb{R}^{p\times 1}$ is the coefficient vector; and $\varepsilon_i^j \in \mathbb{R}^{p\times 1}$ is the residuals vector.

The j^{th} slice can be written as,

$$C_j = \begin{bmatrix} c_1^j(t_1) & c_1^j(t_2) & \cdots & c_1^j(t_p) \\ c_2^j(t_1) & c_2^j(t_2) & \cdots & c_2^j(t_p) \\ \vdots & \vdots & \ddots & \vdots \\ c_q^j(t_1) & c_q^j(t_2) & \cdots & c_q^j(t_p) \end{bmatrix}_{q\times p}, \qquad (3)$$

and the whole brain data as,

$$C = [C^1 \quad C^2 \quad \cdots \quad C^M]_{q\times p\times M}. \qquad (4)$$

The objective of CorrCA is to find a linear combination of the p measurements (y_i^j), defined as,

$$\hat{y}_i^j(t) = V^{\boldsymbol{T}} x_i^j, \qquad (5)$$

such that the correlation across M slices is maximized — where $V \in \mathbb{R}^{p\times 1}$ is a projection vector. The projection matrix V is a set of eigen vectors referred to as correlated components. They are such that the first component corresponds to the direction of maximum correlation across M slices, i.e. (largest ISC). The second component correspond to the direction with second largest ISC and so forth, until the last component which corresponds to the direction with the least ISC.

In matrix format, (2) can be written as,

$$X|_{p\times q\times M} = \left(A|_{p\times k}\right)\left(Y|_{k\times q\times M}\right) + \varepsilon|_{p\times q\times M}. \qquad (6)$$

The least-squares estimate of A is,

$$\hat{A} = R_W V (V^T R_W V)^{-1}. \qquad (7)$$

R_W is the within-slice covariance matrix, which together with the between-slice covariance matrix, R_B, defines the ISC (ρ) as,

$$\rho = \frac{1}{M-1}\frac{V^T R_B V}{V^T R_W V}. \qquad (8)$$

The covariance matrices R_W and R_B are given by,

$$R_W = \sum_{i=1}^{q}\sum_{j=1}^{M}\left(x_i^j - \bar{x}_*^j\right)\left(x_i^j - \bar{x}_*^j\right)^T \quad (9)$$

$$R_B = \sum_{i=1}^{q}\sum_{j=1}^{M}\sum_{k=1,k\neq j}^{M}\left(x_i^j - \bar{x}_*^j\right)\left(x_i^k - \bar{x}_*^k\right)^T. \quad (10)$$

Analogous to using only a few principal components in PCA, here, using only the first few k ($k \leq p$) correlated components with the highest ISC values in (6) and (7), denoised tTACs can be estimated as per (2) as,

$$\hat{C} = \hat{A}\hat{Y}. \quad (11)$$

In short, it can be inferred that CorrCA performs PCA on the matrix of the ratio of between-slices to within-slices, $R_B(R_W)^{-1}$, of which the eigenvalues define the ISC. In this study, the tTACs were denoised with only two components.

CorrCA was computed using the MATLAB codes provided by Parra and colleagues [19], available at *http://parralab.org/corrca*.

III. PROCEDURE

The study was conducted for both simulation and clinical data. A set of voxel-based gray matter simulation data mimicking ^{11}C Pittsburgh compound B (^{11}C-PiB) were used. This is because the clinical data analysed in this study are of the same radiotracer. ^{11}C-PiB reversibly binds to beta amyloid (Aβ) plaques in the brain, and the Aβ plaques are associated with Alzheimer's disease (AD).

Eleven noise-free tTACs representing 11 known *DVR* values were formed. Statistical noise was added to these noise-free tTACs, then for each noise-free tTAC, 1024 noisy tTACs were formed. The *DVR* values were then re-estimated from the noisy tTACs by three methods, LSC-CorrCA, LSC and OLS. Simulation parameters are similar to those used in [16].

Clinical data consisted of ^{11}C-PiB PET data of a cohort of 11 Aβ-negative subjects. The scan was carried out for 70 min in 25 frames (6 × 10 s, 3 × 20 s, 2 × 1 min, 2 × 3 min, and 12 × 5 min). *DVR* parametric images were then obtained from the dynamic PET images by three methods, LSC-CorrCA, LSC, and OLS.

These ^{11}C-PiB parametric images were compared in terms of the contrast between the four main gray matter cortices (frontal, temporal, occipital, and parietal) and white matter (corona radiata). Cerebellum gray matter region was used for the reference region.

The contrast was calculated as [15]:

$$C = \frac{\mu_W - \mu_G}{\sigma_W - \sigma_G}, \quad (12)$$

where μ_G and μ_W respectively represent the mean *DVR* of the gray and white matter regions, and alike, σ_G and σ_W respectively represent the standard deviations of *DVR* in the gray and white matter regions.

IV. RESULTS AND DISCUSSION

Fig. 1 shows an example of a simulated noise-free tTAC, a corresponding noisy tTAC and the corresponding CorrCA-denoised tTAC. It can be seen that the denoised tTACs are almost similar to the noise-free tTAC, indicating the efficiency of CorrCA denoising.

In Fig. 2, the three methods are compared in terms of average *DVR* recovered from the noisy tTACs. A 100% would mean that the method is unbiased. Here, we see that the LSC-CorrCA estimates are as less biased as the LSC estimates. The advantage of LSC-CorrCA is highlighted in this figure, in which LSC-CorrCA estimates shows the smallest deviations in the estimates, based on which the parametric images are expected to be less noisy compared to those of LSC.

Fig. 3 compares the average grey-white matter contrast, calculated for 11 Aβ-negative subjects, of *DVR* images obtained by the three methods. We see that the LSC-CorrCA method gives the highest contrast values. Further, the Friedman post-hoc multiple comparison p-values of the contrast comparison are 0.001 and < 0.001 for LSC-CorrCA compared to LSC and OLS. We can therefore say that LSC-CorrCA has significantly improved the contrast of *DVR* parametric images.

In Fig. 4 we can visually see the difference between the *DVR* images obtained by the three methods. OLS images shows low *DVR* estimates, confirming the underestimation. LSC images shows high *DVR* estimates (compared to OLS), with slight noise components. LSC-CorrCA shows the highest *DVR* estimates, and the noise components that are in LSC images cannot be seen in LSC-CorrCA images —in agreement with all Figs 1 – 3.

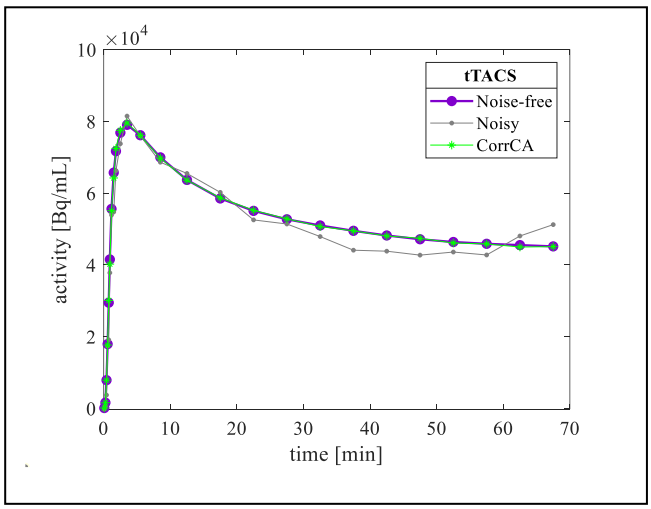

Figure 1. An example of simulated noisy tTAC, and the corresponding noise-free tTAC, as well as the CorrCA-denoised tTAC.

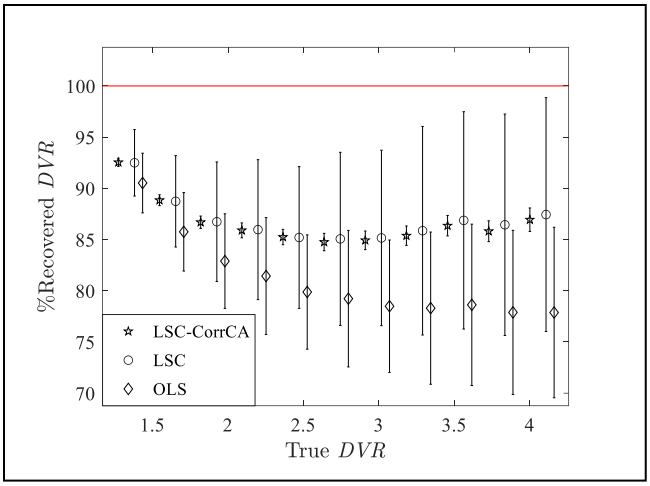

Figure 2. The recovered percentage of the average (N = 1024) *DVR* values estimated from noisy tTACs using the three methods, LSC-CorrCA, LSC, and OLS. The error bars show the standard deviations.

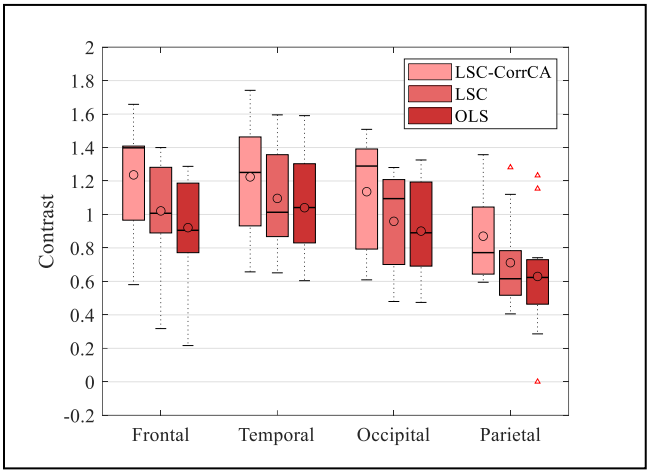

Figure 3. Box plots of the average contrast between grey matter cortices, Frontal, Temporal, Occipital and Parietal, and white matter, Coronal cortex, calculated the 11 Aβ-negative subjects.

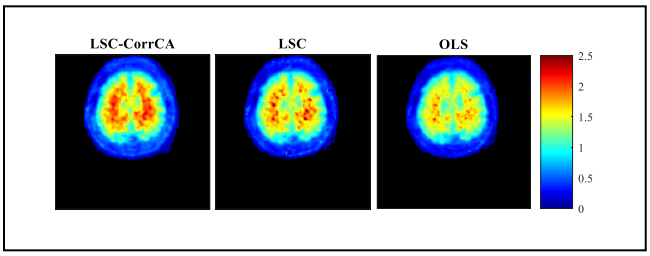

Figure 4. Slices of *DVR* parametric images of an Aβ-negative subject, as obtained by the three methods.

V. CONCLUSION

The results of the method employed in this study, LSC-CorrCA, showed reduced variance in the *DVR* estimates for simulation results. In clinical data, in Fig. 4, improved *DVR* images were obtained for LSC compared to both LSC and OLS. Specifically, the LSC-CorrCA images gave high contrast values, and show a smooth distribution of *DVR* across the slice, with no noise components as those seen in LSC-based images. These results could be significant for quantitative analysis of Aβ in AD patients. The combination of LSC and PCA (LSC-PCA) has been conducted in [16]. Future work will assess the performance of LSC-CorrCA and LSC-PCA.

REFERENCES

[1] J. Logan, J. S. Fowler, N. D. Volkow, G-J J. Wang, Y-J S. Ding, D. L. Alexoff, "Distribution volume ratios without blood sampling from graphical analysis of PET data," *J Cereb Blood Flow Metab.,* 1996, vol. 16(5), pp. 834–40.

[2] J. Logan, J. S. Fowler, N. D Volkow, A. P. Wolf, S. L. Dewey, D. J. Schlyer, R. R. MacGregor, R. Hitzemann, B. Bendriem, S. J. Gatley, et al., "Graphical analysis of reversible radioligand binding from time—activity measurements applied to [N-11C-methyl]-(−)-cocaine PET studies in human subjects," *J Cereb Blood Flow Metab.,* 1990, vol. 10(5), pp. 740–7.

[3] Y. Kimura, M. Naganawa, M. Shidahara, Y. Ikoma, and H. Watabe, "PET kinetic analysis—pitfalls and a solution for the logan plot," *Ann Nucl Med* 2007, vol. 21(1), pp. 1–8.

[4] J. Logan, "A review of graphical methods for tracer studies and strategies to reduce bias," *Nucl Med Biol*, 2003, vol. 30(8), pp. 833–44.

[5] M. Slifstein and M. Laruelle, "Effects of statistical noise on graphic analysis of PET neuroreceptor studies," *J Nucl Med*, 2000, vol. 41(12), pp. 2083–2088.

[6] M. Ichise, H. Toyama, R. B. Innis, and R. E. Carson, "Strategies to improve neuroreceptor parameter estimation by linear regression analysis," *J Cereb Blood Flow Metabol*, 2002, vol. 22(10), pp. 1271–1281.

[7] J. Logan, J. S. Fowler, N. D. Volkow, Y-J S. Ding, G-J. Wang G-J, and D. L. Alexoff," A strategy for removing the bias in the graphical analysis method," *J Cereb Blood Flow Metab*, 2001, vol. 21(3), pp. 307–320.

[8] M. Ichise, J-S. Liow, J-Q. Lu, A. Takano, K. Model, H. Toyama, T Suhara, K. Suzuki, R. B. Innis, and Carson RE, "Linearized reference tissue parametric imaging methods: application to [11 C] DASB positron emission tomography studies of the serotonin transporter in human brain," *J Cereb Blood Flow Metabol*, 2003, vol. 23(9), pp. 1096–1112.

[9] J. Varga and Z. Szabo, "Modified regression model for the logan plot," *J Cereb Blood Flow Metab*, 2002, vol. 22(2), pp. 240–244.

[10] P. K. Shigwedha, T. Yamada, K. Hanaoka, K. Ishii, Y. Kimura, and Y. Fukuoka, "A strategy to account for noise in the X-variable to reduce underestimation in Logan graphical analysis for quantifying receptor density in positron emission tomography," *BMC Medical Imaging*, 2020, vol. 20, Article# 15, pp. 1–8.

[11] D. York, "Least-squares fitting of a straight line," *Can J Phys*, 1966, vol. 44(5), pp. 1079–1086.

[12] D. York, "Least squares fitting of a straight line with correlated errors," *Earth Planet Sci Lett*., 1968, vol. 5, pp. 320–324.

[13] D. York, N. M. Evensen, M. L. Martínez, and J. De Basabe Delgado, "Unified equations for the slope, intercept, and standard errors of the best straight line," *Am J Phys*, 2004, vol. 72(3), pp. 367–375.

[14] L. C. Parra, S. Haufe, and J. P. Dmochowski, "Correlated components analysis-extracting reliable dimensions in multivariate data," *arXiv preprint arXiv:1801.08881*, 2018.

[15] T. Yamada, Y. Kimura, K. Fujii, S. Watanabe, T. Nagaoka, M. Nemoto, K. Hanaoka, H. Kaida, C. Hosokawa, and K. Ishii, "Noise reduction algorithm for amyloid imaging preserving image resolution —quantitative evaluation using clinical images," *Human Amyloid Imaging Conference*, 2018.

[16] P. K. Shigwedha, T. Yamada, K. Hanaoka, K. Ishii, Y. Kimura, and Y. Fukuoka, "Improving contrast between gray and white matter of Logan graphical analysis' parametric images in positron emission tomography through least-squares cubic regression and principal component analysis*," Biomedical Physics & Engineering Express*, vol. 7(3), 035003, 2021.